Possible connection between the optimal path and flow in percolation clusters

Eduardo López,[1] Sergey V. Buldyrev,[1,2] Lidia A. Braunstein,[1,3] Shlomo Havlin,[4] and H. Eugene Stanley[1]

[1]*Center for Polymer Studies, Boston University, Boston, Massachusetts 02215, USA*

[2]*Department of Physics, Yeshiva University, 500 W 185th Street, New York, New York 10033, USA*

[3]*Departamento de Física, Facultad de Ciencias Exactas y Naturales, Universidad Nacional de Mar del Plata, Funes 3350,*
7600 Mar del Plata, Argentina

[4]*Minerva Center & Department of Physics, Bar-Ilan University, Ramat Gan, Israel*

We study the behavior of the optimal path between two sites separated by a distance r on a d-dimensional lattice of linear size L with weight assigned to each site. We focus on the strong disorder limit, i.e., when the weight of a single site dominates the sum of the weights along each path. We calculate the probability distribution $P(\ell_{opt}|r,L)$ of the optimal path length ℓ_{opt}, and find for $r \ll L$ a power-law decay with ℓ_{opt}, characterized by exponent g_{opt}. We determine the scaling form of $P(\ell_{opt}|r,L)$ in two- and three-dimensional lattices. To test the conjecture that the optimal paths in strong disorder and flow in percolation clusters belong to the same universality class, we study the tracer path length ℓ_{tr} of tracers inside percolation through their probability distribution $P(\ell_{tr}|r,L)$. We find that, because the optimal path is not constrained to belong to a percolation cluster, the two problems are different. However, by constraining the optimal paths to remain inside the percolation clusters in analogy to tracers in percolation, the two problems exhibit similar scaling properties.

I. INTRODUCTION

Flow in porous media, due to its ubiquitous nature, has received a great deal of attention in recent decades [1–5]. Interest has been driven by multiple real-world problems such as oil extraction [4,5] and ground water pollution [6,7]. Porous media is typically simulated through percolation systems [8], and flow through a variety of models ranging from the idealized ant in a labyrinth [9] to the very practical ones such as convective tracer flow [5,10,11].

In the study of flow in percolation clusters, it has been hypothesize that transport properties may be related to some geometric property of the cluster. However, despite considerable effort [1] such a geometric property relation has not been found [2]. Here, we argue that, for the particular case of convective tracer flow in percolation clusters, a connection exists between transport properties and the static properties of a model of optimal paths in disordered lattices, described in detail below. This relation allows for a mapping between the two problems that opens new approaches for their study.

The first hint of a possible connection between flow in porous media and the optimal path problem arouse in the work of Lee and co-workers [12]. This reference deals with a simplified model of flow in porous media related to secondary oil extraction, in which an invading fluid (water, steam, etc.) injected at A pushes oil out through extraction well B. This method is used when the oil reservoir does not have enough pressure to be exploited without this added driving pressure. The system is considered in the following way: the medium is modeled by a percolation cluster at the critical threshold density, and a steady state laminar flow of an incompressible fluid is established between A and B. Then, tracers which mimic the flow of the driving fluid are injected at A and travel purely by convection to B (Sec. III). The tracer length (ℓ_{tr}) probability density function (PDF), $P(\ell_{tr})$, was measured and it was found that the most probable trav-

eling length ℓ_{tr}^*, defined as the value of ℓ_{tr} for which $P(\ell_{tr})$ is maximum, scales with the distance r between the injection and extraction sites A and B as

$$\ell_{tr}^* \sim r^{d_{tr}} \quad [d_{tr} = 1.21 \pm 0.02 \text{ for } d=2]. \tag{1}$$

The remarkable feature of Eq. (1) is that, for $d=2$, the exponent $d_{tr} \approx d_{opt}$, where d_{opt} is the exponent for the optimal path length in the strong disorder limit as defined by Cieplak and co-workers [13,14] (see below). In this study, we propose that transport in percolation can be directly related to the optimal path in strong disorder, and we support our proposal with extensive numerical simulations for d-dimensional lattices with $d=2$ and 3.

The optimal path problem formulated by Cieplak and co-workers in Ref. [13] is that of finding the path of lowest cost to go from one end of a d-dimensional lattice to the other end when to each site (or bond) i, we associate a weight $\epsilon_i = e^{ax_i}$, with $x_i \in [0,1)$. This is equivalent to choosing ϵ_i from the distribution

$$W(\epsilon) = \frac{1}{a\epsilon} \quad \epsilon \in [1, \exp a]. \tag{2}$$

The energy of any path of length ℓ on the lattice is given by the sum

$$E \equiv \sum_{j}^{\ell} \epsilon_j, \tag{3}$$

where j is an index running over the sites of the path. The limit $a \to \infty$ is known as the strong disorder limit. The optimal path of length ℓ_{opt} is the path for which E is minimal with respect to all other paths. The optimal path length scales with r as [13]

$$\ell_{\text{opt}} \sim r^{d_{\text{opt}}} \quad [d_{\text{opt}} = 1.22 \pm 0.01]. \tag{4}$$

The first reference that we have found to this problem, although formulated in a different context, is that of Ambegaokar and co-workers [15], where the metal-insulator transition is considered by a percolation model in which sites represent possible electron states which can be reached only by hopping through quantum tunneling, and the hopping rates are exponential, motivating Eq. (2). Another context in which these weights have been observed is that of magnetoresistance in thin Ni films [16].

Our work can be equated to the following question: is flow in percolation clusters, a dynamical process, connected to the optimal path length in strong disorder, a static property, as suggested by the similarity of Eqs. (1) and (4)? To this end, we study the PDF $P(\ell_{\text{opt}}|r,L)$ for the optimal path to have a length ℓ_{opt}, given a system size L, and an Euclidean distance r between the starting and ending sites A and B of the path. We will compare this PDF with $P(\ell_{\text{tr}}|r,L)$, the PDF that convective tracer paths have a length ℓ_{tr} in a percolation system of size L at criticality, where the starting and ending sites are at a distance r.

There are some indications that this connection is indeed present, given that other relations between percolation and strong disorder optimal paths have been reported. For instance, for a lattice with disorder given by Eq. (2) in the strong disorder limit, the most probable largest weight of the site used by the optimal path is e^{ap_c}, where p_c is the percolation threshold [14]. Also, Wu and co-workers [17] recently determined through the study of tracer flow on a lattice with disorder, that the strong disorder limit has a length scale that scales as a^ν, where ν is the connectedness exponent of percolation [3], and hence a system is in the strong disorder limit only when $a^\nu > L$. In this paper, we study the ultrametric limit $a \to \infty$.

In Sec. II we present results for the distribution $P(\ell_{\text{opt}}|r,L)$. In Sec. III, results for $P(\ell_{\text{tr}}|r,L)$ are presented and compared with $P(\ell_{\text{opt}}|r,L)$. We then discuss the results in Sec. IV.

II. OPTIMAL PATH DISTRIBUTION

To study $P(\ell_{\text{opt}}|r,L)$ we use the "bombing algorithm" proposed in Ref. [13]. The optimal path length ℓ_{opt} between sites A and B is found by eliminating (bombing) sites of the lattice in decreasing order of weight, but leaving those sites necessary to keep A and B connected. When all sites that do not disconnect A and B are eliminated, only the sites of the optimal path remain [18–20].

In Fig. 1 we present $P(\ell_{\text{opt}}|r,L)$ for $r \ll L$ for a square lattice of sites. Four distinct features appear:

(1) The most probable optimal path length ℓ_{opt}^* scales with r as

$$\ell_{\text{opt}}^* \sim r^{d_{\text{opt}}}. \tag{5}$$

The values of d_{opt} have been reported for several lattice dimensions d, and also have been shown to be universal [21]. Here, we rescale $P(\ell_{\text{opt}}|r,L)$ with the exponent d_{opt}, calculated elsewhere for the average optimal path length
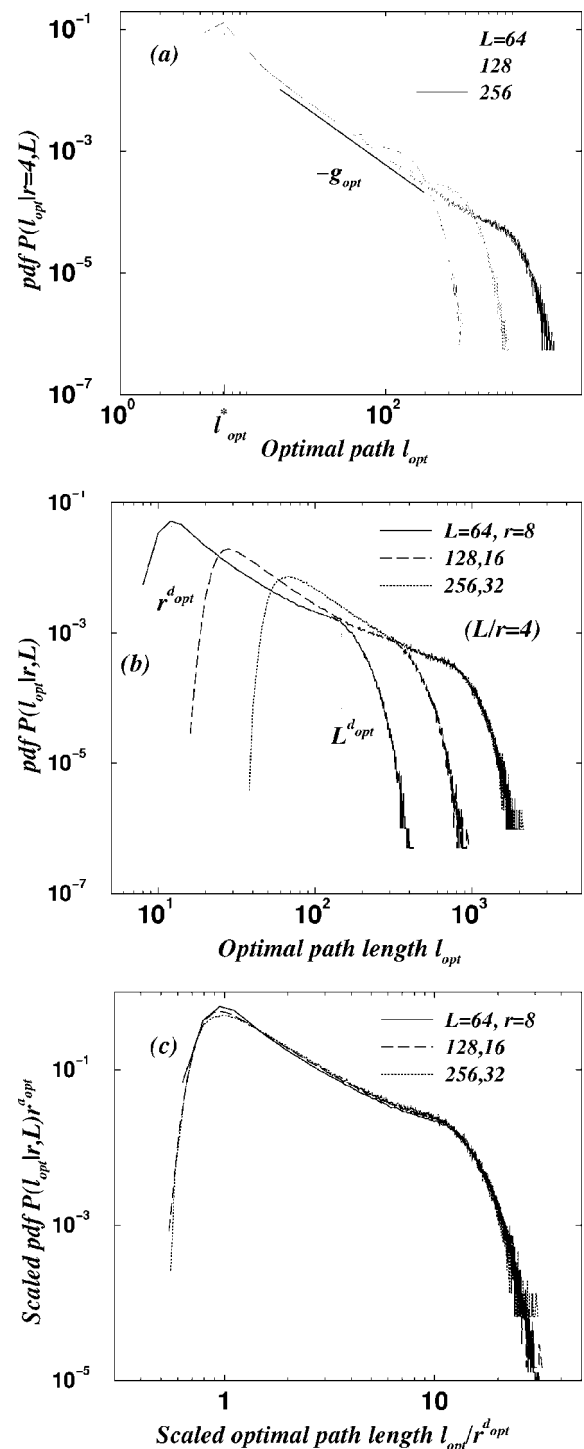

FIG. 1. (a) Distribution $P(\ell_{\text{opt}}|r,L)$ for $r=4$ and system sizes $L=64,, 128,$ and 256. As L increases, the power law region with exponent g_{opt} becomes better defined, and the upper cutoff increases. (b) Probability distribution $P(\ell_{\text{opt}}|r,L)$ for $(r=8,L=64)$ (solid line), $(r=16,L=128)$ (dashed line), and $(r=32,L=256)$ (dotted line) for two-dimensional systems. The ratio between L and r is kept fixed for these curves. (c) Scaled distribution $r^{d_{\text{opt}}}P(\ell_{\text{opt}}|r,L)$ vs scaled optimal path length $\ell_{\text{opt}}/r^{d_{\text{opt}}}$ for the curves in (b). The collapse has been achieved using the exponent d_{opt} reported for $\bar{\ell}_{\text{opt}}$, which is also valid for the most probable length ℓ_{opt}^* as evidenced in the plot.

TABLE I. Exponents characterizing $P(\ell_{\text{opt}}|r,L)$ and $P(\ell_{\text{tr}}|r,L)$, which are defined in the text. The value of g_{opt} is determined from $P(\ell_{\text{opt}}|r=4,L=256)$ in Fig. 1(a), for which the power-law region is the longest. The values of ϕ_{opt} and ψ_{opt} are from Fig. 2.

		Optimal path in strong disorder ("Static")			
d	d_{opt}	g_{opt}	ϕ_{opt} (calculated)	$\phi_{\text{opt}} = \dfrac{1}{d_{\text{opt}} - 1}$	ψ_{opt} (calculated)
2	1.22 ± 0.01 [13,21]	1.55 ± 0.05	4.8 ± 0.5	4.55 ± 0.21	5.3 ± 0.3
3	1.42 ± 0.02 [27]	1.37 ± 0.05	2.1 ± 0.1	2.3 ± 0.1	4.3 ± 0.3
		Optimal path in strong disorder inside percolation ("Modified static")			
2	1.21 ± 0.02	1.82 ± 0.05	4.9 ± 0.4	4.76 ± 0.45	2.3 ± 0.4
3	1.40 ± 0.03	2.2 ± 0.1	2.0 ± 0.1	2.5 ± 0.2	3.6 ± 0.2
		Tracer path ("dynamic")			
d	d_{tr}	g_{tr}	ϕ_{tr} (calculated)	$\phi_{\text{tr}} = \dfrac{1}{d_{\text{tr}} - 1}$	ψ_{tr} (calculated)
2	1.21 ± 0.02 [12]	1.82 ± 0.05	4.7 ± 0.4	4.76 ± 0.45	2.7 ± 0.2
3	1.37 ± 0.05	2.23 ± 0.09	1.81 ± 0.02	2.7 ± 0.4	3.46 ± 0.04

$\bar{\ell}_{\text{opt}}$, but, as Figs. 1(a) and 1(b) show, d_{opt} also produces the correct scaling for ℓ_{opt}^*. Our results for d_{opt} are reported in Table I for $d=2$ and 3.

(2) A lower cutoff [Fig. 1(b)] which, in analogy with the distribution of minimal paths in percolation [4,22,23], is expected to be a stretched exponential function f_1 of the form

$$f_1(x) = \exp(-\alpha x^{-\phi_{\text{opt}}}) \quad \left[x \equiv \frac{\ell_{\text{opt}}}{r^{d_{\text{opt}}}} \right], \quad (6)$$

where α is a lattice-dependent constant, and ϕ_{opt} is a universal exponent satisfying [21,22]

$$\phi_{\text{opt}} = \frac{1}{d_{\text{opt}} - 1}. \quad (7)$$

(3) An upper cutoff due to the effect of the finite lattice size L. A stretched exponential behavior is also expected to describe this region [4,19,23], through a function f_2 of the form

$$f_2(y) = \exp(-\beta y^{\psi_{\text{opt}}}) \quad \left[y \equiv \frac{\ell_{\text{opt}}}{L^{d_{\text{opt}}}} \right], \quad (8)$$

where β is a lattice-dependent constant, and ψ_{opt} has universal properties [4,19,23].

(4) A power-law region described by

$$P(\ell_{\text{opt}}) \sim \ell_{\text{opt}}^{-g_{\text{opt}}} \quad [r^{d_{\text{opt}}} < \ell_{\text{opt}} \leqslant L^{d_{\text{opt}}}]. \quad (9)$$

The above considerations lead us to postulate for $P(\ell_{\text{opt}}|r,L)$ a full scaling ansatz [4,21–23]

$$P(\ell_{\text{opt}}|r,L) \sim \frac{1}{r^{d_{\text{opt}}}} \left(\frac{\ell_{\text{opt}}}{r^{d_{\text{opt}}}} \right)^{-g_{\text{opt}}} f_1\left(\frac{\ell_{\text{opt}}}{r^{d_{\text{opt}}}} \right) f_2\left(\frac{\ell_{\text{opt}}}{L^{d_{\text{opt}}}} \right), \quad (10)$$

where the prefactor $1/r^{d_{\text{opt}}}$ is necessary for normalization. We have tested this ansatz for $d=2,3$ and found it to be consistent with our earlier simulations [21].

An interesting feature of $P(\ell_{\text{opt}}|r,L)$ is that, as d increases, g_{opt} decreases. In other words, the longer optimal paths at larger dimensions have a larger probability (see Table I). Additionally, since $g_{\text{opt}}<2$ for all d, $\bar{\ell}_{\text{opt}}$ and all higher moments diverge as $L\to\infty$.

To calculate the exponents ϕ_{opt} and ψ_{opt} of Eqs. (6) and (8), we introduce the function

$$\Pi\left(\frac{\ell_{\text{opt}}}{r^{d_{\text{opt}}}}, \lambda, A \right) \equiv \ln\left[\frac{A}{P(\ell_{\text{opt}}|r,L)r^{d_{\text{opt}}}\left(\dfrac{\ell_{\text{opt}}}{r^{d_{\text{opt}}}} \right)^{g_{\text{opt}}}} \right] \quad (11)$$

which, upon using Eqs. (6), (8), and (10) yields

$$\Pi\left(\frac{\ell_{\text{opt}}}{r^{d_{\text{opt}}}}, \lambda, A \right) \sim \ln\left[\frac{A}{f_1\left(\dfrac{\ell_{\text{opt}}}{r^{d_{\text{opt}}}} \right) f_2\left(\dfrac{\ell_{\text{opt}}}{r^{d_{\text{opt}}}}\lambda^{-d_{\text{opt}}} \right)} \right] \sim \ln A$$

$$+ \alpha\left(\frac{\ell_{\text{opt}}}{r^{d_{\text{opt}}}} \right)^{-\phi_{\text{opt}}} + \beta\left(\frac{\ell_{\text{opt}}}{r^{d_{\text{opt}}}}\lambda^{-d_{\text{opt}}} \right)^{\psi_{\text{opt}}}.$$

$$(12)$$

We have made use of $\lambda \equiv L/r$ in the argument of the function f_2 so that $f_2(\ell_{\text{opt}}/L^{d_{\text{opt}}})=f_2(\lambda^{-d_{\text{opt}}}\ell_{\text{opt}}/r^{d_{\text{opt}}})$. The constant A is an auxiliary parameter chosen to make the minimum value of Π slightly larger than unity. Defining $x \equiv \ell_{\text{opt}}/r^{d_{\text{opt}}}$, we show in Fig. 2 $\Pi(x,\lambda,A)$ for $d=2$ and the fit lines for the exponents of both f_1 and f_2, which are reported in Table I. The
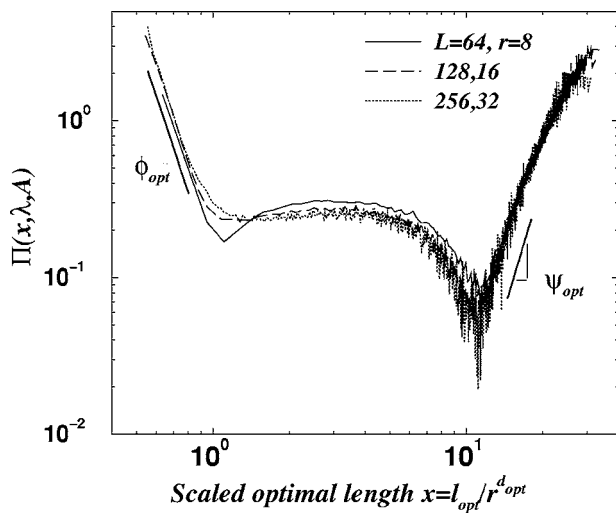
FIG. 2. The scaling function $\Pi(x,\lambda,A)$ for $A=0.1$ vs the scaled optimal path length $x \equiv \ell_{opt}/r^{d_{opt}}$ for system sizes $(r=8,L=64)$, $(r=16,L=128)$, and $(r=32,L=256)$. The two straight lines serve as guides to the eye for the data that determine the exponents ϕ_{opt} and ψ_{opt}.

values of ϕ_{opt} we calculate are close to the values predicted by Eq. (7) for $d=2,3$.

III. COMPARISON BETWEEN FLOW IN PERCOLATION AND THE OPTIMAL PATH

We now study the PDF $P(\ell_{tr}|r,L)$ with the purpose of comparing it to $P(\ell_{opt}|r,L)$, and analyze the detailed conditions under which optimization and flow in percolation occur. Our analysis (see Sec. IV) explains the differences we observe, and also the "right way" in which the two problems become equivalent.

Since simulations for flow on percolation clusters are performed, we describe the two-dimensional case of the algorithm [5]. We represent the reservoir as a two-dimensional site percolation cluster, and choose sites at $(-r/2,0)$ and $(r/2,0)$, denoted by A and B, respectively, to be the injection and extraction well positions. Points A and B are separated by a geometric distance r, and the system box has corners at $(\pm L/2,\pm L/2)$. We construct percolation clusters at p_c using the Leath algorithm [24].

To model tracer motion we use the analogy with electrical circuits, where for each bond, the pressure drop corresponds to the voltage difference, and the flow corresponds to the electrical current on the bond. A pressure difference between sites A and B drives the tracer. For each realization, 10^4 tracers are introduced at site A, and then collected at site B. The set of all sites through which there is a nonzero current defines the cluster backbone of M_B sites.

The "pressure" difference across bonds is equivalent to a "voltage" difference, so by solving Kirchhoff's equations on the backbone, we obtain the potential (pressure) drops ΔV over all bonds for a given realization. Due to the nature of the model, no turbulence or other complex fluid flow effects are considered, which is equivalent to assuming laminar flow
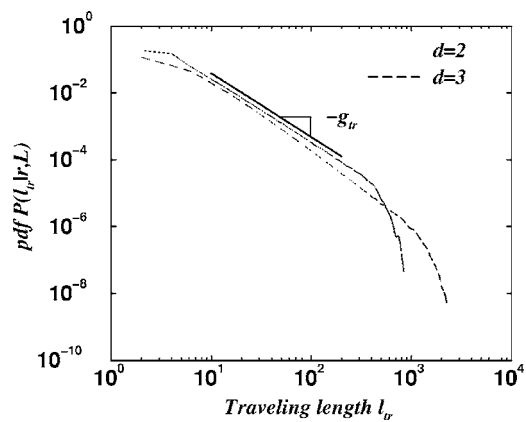
inside the system. Additionally, given that the bonds have vanishing radius, the tracer flow "perfectly mixes" at the nodes. For site i having s_i outgoing bonds, the tracer selects a bond with a probability

$$w_{ij} \equiv \frac{\Delta V_{ij}}{\sum_j \Delta V_{ij}} \quad [j=1,\dots,s_i; i=1,\dots,M_B]. \quad (13)$$

For incoming bonds, $w_{ij}=0$. This guarantees that the tracer dynamics is completely convective, i.e., with infinite Péclet number [25,26]. The total traveling length of a tracer is the number of bonds of the path connecting A and B, chosen by this tracer. Since the particles do not interact with one another, it is equivalent to launching one particle at a time into the cluster. This procedure is known as *particle launching algorithm* [10,11]. We determine the probability distribution
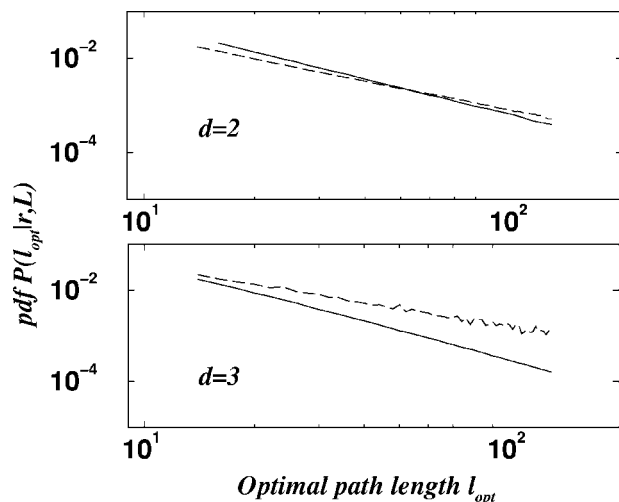

FIG. 3. Probability distribution $P(\ell_{tr}|r,L)$ for $r=2$ and $L=128$ in $d=2$ and $d=3$. In a similar fashion as for $P(\ell_{opt}|r,L)$ we see a power-law region that we characterize by exponent g_{tr}. Another feature of this plot is the increasing steepness of $P(\ell_{tr}|r,L)$ as d increases (implying g_{tr} increases with d), a feature for which $P(\ell_{opt}|r,L)$ has the opposite behavior, as g_{opt} decreases with d.

FIG. 4. The power-law tails of $P(\ell_{tr}|r,L)$ (solid) and $P(\ell_{opt}|r,L)$ (dashed) in $d=2$ and 3. The upper pair is for $d=2$ with $L=256$ and $r=4$. The lower pair is for $d=3$ with $L=128$ and $r=2$.
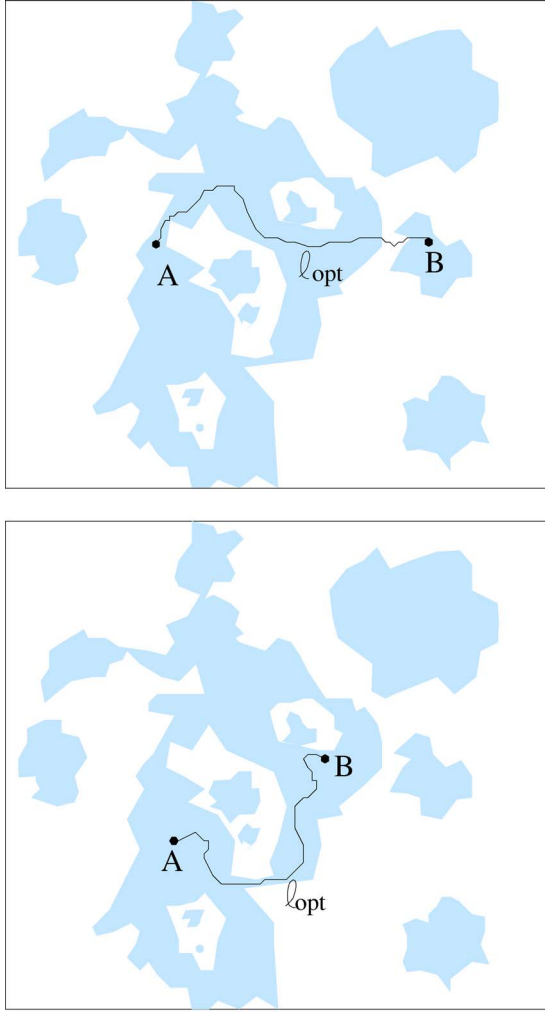
FIG. 5. (Color online) (a) Schematic of occupied sites for p below the percolation threshold p_c, and the optimal path in strong disorder. The darker regions represent sites that are still present when p_c is reached. We see in this case that ℓ_{opt} must cross the region above p_c (i.e., leave the cluster) to connect A and B. (b) If sites A and B are chosen within the a cluster below p_c, the optimal path does not leave the cluster because that would increase the cost.

of the tracer traveling lengths $P(\ell_{tr}|r,L)$ by counting the number of particles that travel from site A to site B along a path of length ℓ_{tr}, over all the particles and all realizations of the percolation cluster.

The form of $P(\ell_{tr}|r,L)$ for the two-dimensional case was suggested in [12]. Here, we extend these results to $d=3$ (Fig. 3). Once again, the power law and stretched exponential behaviors are present. The scaling of the most probable tracer path length is given by $\ell_{tr}^* \sim r^{d_{tr}}$. These results yield

$$P(\ell_{tr}|r,L) \sim \frac{1}{r^{d_{tr}}} \left(\frac{\ell_{tr}}{r^{d_{tr}}}\right)^{-g_{tr}} h_1\left(\frac{\ell_{tr}}{r^{d_{tr}}}\right) h_2\left(\frac{\ell_{tr}}{L^{d_{tr}}}\right), \quad (14)$$

where functions h_1 and h_2 have the forms

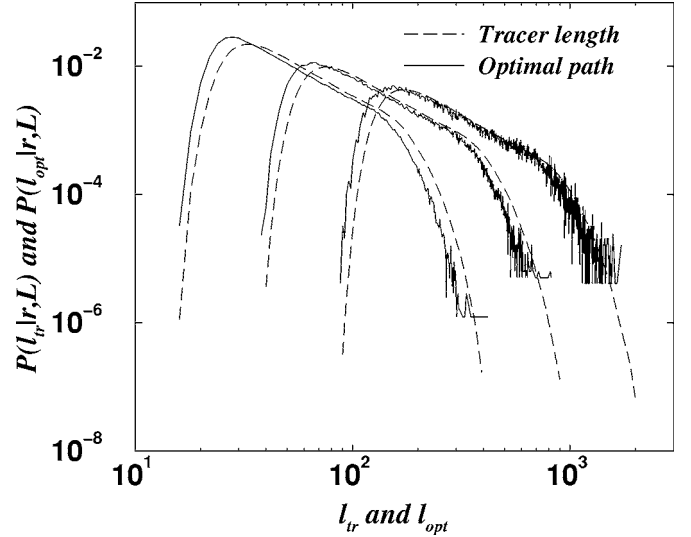$$h_1(z) = \exp(-\mu z^{-\phi_{tr}}) \quad \left[z \equiv \frac{\ell_{tr}}{r^{d_{tr}}}\right], \quad (15)$$

and

FIG. 6. Comparison of $P(\ell_{opt}|r,L)$ inside percolation with $P(\ell_{tr}|r,L)$ for $(r=16,L=64)$, $(r=32,L=128)$ and $(r=64,L=256)$. The solid lines represent the optimal path distribution, and the long dashed lines the tracer length distributions. The values of r and L have a fixed ratio equal to $L/r=4$. The similarity between distributions is clear, supporting our hypothesis. The small separation along the horizontal axis between $P(\ell_{opt}|r,L)$ and $P(\ell_{tr}|r,L)$ (consistent for the three pairs of curves) is due to nonuniversal details of the two models.

$$h_2(u) = \exp(-\rho u^{\psi_{tr}}) \quad \left[u \equiv \frac{\ell_{tr}}{L^{d_{tr}}}\right]. \quad (16)$$

Arguments similar to those leading to Eq. (12) indicate how to determine the exponents ϕ_{tr} and ψ_{tr}, reported in Table I.

The power-law region is characterized by the exponent g_{tr}, which is different from g_{opt} (see Table I). We present in Fig. 4 curves for the power-law regime for both $P(\ell_{tr}|r,L)$ and $P(\ell_{opt}|r,L)$ in $d=2$ and 3. In Table I we see the difference in the slope of the power-law decay between $P(\ell_{tr}|r,L)$ and $P(\ell_{opt}|r,L)$. Moreover, as d increases, g_{opt} decreases and g_{tr} increases, indicating the differing behaviors for the two problems. In the next section, we explain the origin of the differences, how these differences can be removed, and under which conditions the two problems coincide.

IV. DISCUSSION

The numerical results presented above show the difference in the values of the scaling exponents g_{opt} and g_{tr} of the distributions. To understand these differences, we now elaborate on the characteristics of the optimal path problem in comparison to those of tracer paths in percolation.

In Fig. 5(a) we represent the optimal path in strong disorder, where the dark areas represent regions with site weights $\epsilon_i = e^{ax_i}$ with $x_i \lesssim p_c$, and the white areas regions with site weights $\epsilon = e^{ax_i}$ with $x_i > p_c$. Typically, the arbitrary choice of A and B may lead to a path connecting them that requires visiting regions with site weights $\epsilon > e^{ap_c}$. In contrast, the tracers inside percolation clusters must, by definition, travel on the *same* percolation cluster (spanning or otherwise), be-

cause the flow takes place only if there is a percolating path between A and B. Therefore, this difference between the flow and optimal path problems presents a possible explanation for the differences between $P(\ell_{opt}|r,L)$ and $P(\ell_{tr}|r,L)$. Optimal paths tend to be longer because they are able to visit more sites of the lattice and are therefore of longer length, whereas tracers in percolation flow are confined to a given cluster, and their traveling lengths are much more limited. These features intuitively explain why g_{tr} is larger than g_{opt}.

The above considerations lead to the following hypothesis: if the optimal path search is constrained to pairs of sites within regions of the lattice that are part of the same cluster [Fig. 5(b)], then the scaling of $P(\ell_{opt}|r,L)$ and $P(\ell_{tr}|r,L)$ would coincide. To test this, we present $P(\ell_{opt}|r,L)$ and $P(\ell_{tr}|r,L)$ in Fig. 6, where the optimal paths satisfy the condition that their highest weight is at or below percolation. This condition forces the optimal paths to be inside percola-

tion clusters. Indeed, for this case (Fig. 6), the two quantities exhibit very similar behavior, supporting our hypothesis. The exponent g_{opt} inside percolation now becomes very close to g_{tr}. On the other hand, d_{opt} does not change, confirming the equivalence of the two problems. We also have similar results for three-dimensional lattices.

In summary, we have shown that $P(\ell_{opt}|r,L)$ has a power-law tail with an exponent g_{opt} which decays as d grows and is different from the power-law tail of $P(\ell_{tr}|r,L)$. This difference seems to be related to the fact that the optimal path crosses percolation clusters and thus tends to have longer lengths compared with tracers which are always inside percolation clusters. When ℓ_{opt} is measured only inside percolation clusters, our results suggest $P(\ell_{opt}|r,L)$ and $P(\ell_{tr}|r,L)$ are equivalent and the two problems possibly belong to the same universality class.

[1] D. ben-Avraham and S. Havlin, *Diffusion and Reactions in Fractals and Disordered Systems* (Cambridge University Press, Cambridge, 2000).

[2] S. Havlin and D. ben-Avraham, Adv. Phys. **36**, 695 (1987), and references therein.

[3] *Fractals and Disordered Systems*, 2nd ed., edited by A. Bunde and S. Havlin (Springer, Berlin, 1996).

[4] J. S. Andrade, S. V. Buldyrev, N. Dokholyan, S. Havlin, P. R. King, Y. Lee, G. Paul, and H. E. Stanley, Phys. Rev. E **62**, 8270 (2000).

[5] E. López, S. V. Buldyrev, N. V. Dokholyan, L. Goldmakher, S. Havlin, P. R. King, and H. E. Stanley, Phys. Rev. E **67**, 056314 (2003).

[6] J. Koplik, S. Redner, and D. Wilkinson, Phys. Rev. A **37**, 2619 (1988).

[7] J.-C. Bacri, J. P. Bouchaud, A. Georges, E. Guyon, J. P. Hulin, N. Rakotomalala, and D. Salin, in *Hydrodynamics of Dispersed Media*, edited by J. P. Hulin, A. M. Cazabat, E. Guyon, and F. Carmona (Elsevier/North-Holland, Amsterdam, 1990), p. 249.

[8] D. Stauffer and A. Aharony, *Introduction to Percolation Theory*, 2nd ed. (Taylor and Francis, London, 1994).

[9] P. G. de Gennes, Recherche **7**, 919 (1976).

[10] J. Koplik, S. Redner, and D. Wilkinson, Phys. Rev. A **37**, 2619 (1988).

[11] M. Sahimi, H. T. Davis, and L. E. Scriven, Chem. Eng. Commun. **23**, 329 (1983); M. Sahimi, A. L. Heiba, B. D. Hughes, L. E. Scriven, and H. T. Davis, Chem. Eng. Sci. **41**, 2103 (1986); **41**, 2123 (1986); M. Sahimi and A. O. Imdakm, J. Phys. A **21**, 3833 (1988).

[12] Y. Lee, J. S. Andrade, S. V. Buldyrev, N. V. Dokholyan, S. Havlin, P. R. King, G. Paul, and H. E. Stanley, Phys. Rev. E **60**, 3425 (1999).

[13] M. Cieplak, A. Maritan, and J. R. Banavar, Phys. Rev. Lett. **72**, 2320 (1994).

[14] M. Porto, S. Havlin, H. E. Roman, and A. Bunde, Phys. Rev. E

58, R5205 (1998).

[15] V. Ambegaokar, B. I. Halperin, and J. S. Langer, Phys. Rev. B **4**, 2612 (1971).

[16] Y. M. Strelniker, R. Berkovits, A. Frydman, and S. Havlin, Phys. Rev. E **69**, 065105(R) (2004).

[17] Z. Wu, E. López, S. V. Buldyrev, L. A. Braunstein, S. Havlin, and H. E. Stanley, Phys. Rev. E **71**, 045101(R) (2005).

[18] L. A. Braunstein, S. V. Buldyrev, S. Havlin, and H. E. Stanley, Phys. Rev. E **65**, 056128 (2002).

[19] S. V. Buldyrev, L. A. Braunstein, R. Cohen, S. Havlin, and H. E. Stanley, Physica A **330**, 246 (2003).

[20] Since most of the computational demands come from checking connectivity between A and B, we use the method in Ref. [19], which consists of finding the shortest path between A and B, and then, as long as none of the sites of this shortest path is bombed, it is not necessary to check connectivity. Only when a site of the shortest path is bombed, connectivity is checked. If there is a new shortest path, the site is eliminated, but if there is no alternative path, then the site belongs to the optimal path and the shortest path is kept.

[21] S. V. Buldyrev, S. Havlin, E. López, and H. E. Stanley, Phys. Rev. E **70**, 035102(R) (2004).

[22] S. Havlin and D. ben-Avraham, Adv. Phys. **36**, 695 (1987).

[23] N. Dokholyan, Y. K. Lee, S. V. Buldyrev, S. Havlin, P. R. King, and H. E. Stanley, J. Stat. Phys. **93**, 603 (1998).

[24] P. L. Leath, Phys. Rev. B **14**, 5046 (1976).

[25] The Péclet number is defined as the ratio between the characteristic length scale times the average fluid velocity, divided by the molecular diffusion coefficient. Infinite Péclet number is equivalent to saying that no diffusion occurs in the system, and the problem is completely convective.

[26] The difusive regime, of great relevance in many systems, does not exhibit any relation to the connection between the convective tracer flow and the optimal path problem that we address.

[27] M. Cieplak, A. Maritan, and J. R. Banavar, Phys. Rev. Lett. **76**, 3754 (1996).